

**NASA
Technical
Paper
3389**

1993

**Generalized Three-Dimensional Simulation
of Ferruled Coupled-Cavity Traveling-
Wave-Tube Dispersion and
Impedance Characteristics**

Joseph W. Maruschek
*Ohio Aerospace Institute
Brook Park, Ohio*

Carol L. Kory
*Analex Corporation
Lewis Research Center
Brook Park, Ohio*

Jeffrey D. Wilson
*Lewis Research Center
Cleveland, Ohio*



National Aeronautics and
Space Administration
Office of Management
Scientific and Technical
Information Program

Trade names or manufacturers' names are used in this report for identification only. This usage does not constitute an official endorsement, either expressed or implied, by the National Aeronautics and Space Administration.

Summary

The frequency-phase dispersion and Pierce on-axis interaction impedance of a ferruled coupled-cavity traveling-wave-tube (TWT) slow-wave circuit were calculated using the three-dimensional simulation code Micro-SOS. The utilization of the code to reduce costly and time-consuming experimental cold tests is demonstrated by the accuracy achieved in calculating these parameters. A generalized input file was developed so that ferruled coupled-cavity TWT slow-wave circuits of arbitrary dimensions could be easily modeled. The practicality of the generalized input file was tested by applying it to the ferruled coupled-cavity slow-wave circuit of the Hughes Aircraft Company model 961HA TWT and by comparing the results with experimental results.

Introduction

Micro-SOS is a three-dimensional electromagnetic circuit analysis code developed by Mission Research Corporation (MRC) in collaboration with Varian Associates as part of a project sponsored by the Department of Defense (DOD) and the National Aeronautics and Space Administration (NASA) to develop computer software for microwave tube design (refs. 1 to 3). Micro-SOS is a version of a larger code, SOS (self-optimized sector), which includes the simulation of charged-particle trajectories. A frequency-domain solver was added to SOS and the particle-handling ability was deleted to form Micro-SOS. The finite-difference code is written in FORTRAN 77 and can be operated in either a time-domain algorithm in which Maxwell's time-dependent equations are solved or in a frequency-domain algorithm in which the resonant mode frequencies and field patterns are obtained. The results described in this report were obtained entirely from simulations using the frequency-domain algorithm of Micro-SOS.

The objectives of the code development were to provide an electromagnetic circuit modeling/analysis capability that was better, faster, and cheaper than that previously available and to provide a means of obtaining more information about the radiofrequency (RF) fields in a circuit than is normally possible through experimental hardware "cold testing." Hardware cold tests refer to evaluating circuit models (actual or scaled) on the RF test bench with no electron beam present.

The cold tests are used to determine the RF phase shift, interaction impedance, and attenuation for a cavity. These data can then be used as input for a coupled-cavity TWT RF-beam-interaction computer model (ref. 4) which simulates the output RF power and beam characteristics.

Using Micro-SOS instead of experimental cold testing to obtain these data has several advantages: significant conservation of labor, time, and cost; efficient exploration of novel circuit structure designs; determination of higher frequency mode information which avoids expensive experimental tests to determine potential RF instabilities in a given circuit (ref. 5).

The practicality and efficiency of the frequency-domain algorithm of Micro-SOS were demonstrated by simulating the frequency-phase dispersion and Pierce on-axis interaction impedance characteristics for a ferruled coupled-cavity slow-wave circuit. The Micro-SOS results obtained for both the dispersion and impedance characteristics are compared in this report to experimental cold-test results. The facility of using the generalized Micro-SOS input file for ferruled coupled-cavity TWT circuits is also shown. By simply replacing the existing dimensions with the dimensions of the circuit of interest, dispersion curves and the Pierce on-axis interaction impedance characteristics can be readily determined for any ferruled coupled-cavity TWT circuit.

Symbols

a_n, b_n, E_n	on-axis axial electric field harmonic magnitude, V/m
$E_{z\text{tot}}$	total on-axis axial electric field, V/m
f	frequency, GHz
g	ferrule gap, m
h	cavity gap, m
K_n	Pierce on-axis interaction impedance, Ω
L	cavity length, m
N	number of cavities in simulation
n	space harmonic order

P	period of $E_{z\text{tot}}$, m
P_{RF}	RF power flow, J/s
r_1	ferrule inner radius, m
r_2	ferrule outer radius, m
r_3	slot inner radius, m
r_4	slot outer radius, m
r_5	cavity radius, m
t	cavity wall thickness, m
v_g	group velocity, m/s
W	electromagnetic energy per unit length, J/m
W_T	total electromagnetic energy, J
z	axial coordinate, m
β	axial phase constant, rad/m
θ	slot arc, deg
ϕ	phase shift per cavity for fundamental harmonic, rad
ω	angular frequency, rad

Background

Micro-SOS was used to model the ferruled coupled-cavity slow-wave circuit of the Hughes Aircraft Company 961HA TWT currently under development (ref. 6). The 961HA, a 59- to 64-GHz TWT for intersatellite communications, was designed to have an overall efficiency exceeding 40 percent over the 5-GHz bandwidth for dual-saturated RF output power levels of 30 and 75 W. The design is a revision of the earlier model, the 961H (ref. 7), which had a slot-mode oscillation problem caused by the interaction of the electron beam with the slot mode at the upper cutoff frequency. When the dimensions of the coupling slot in the 961HA were adjusted to shift the slot mode down in frequency, this problem was resolved (ref. 7).

Two views of the generalized ferruled coupled-cavity circuit are shown schematically in figures 1(a) and (b). The coupling slots are rotated 180° at alternating cavity partition walls. The ferrules, which are the hollow posts surrounding

the beam hole, concentrate the RF electric field in the beam region to increase the interaction impedance of the cavity. The corresponding dimensions of a single cavity of the 961HA TWT are listed in table I. The circuit implements 169 cavities over 3 sections with a mild two-stage velocity taper in the output section (ref. 6).

TABLE I.—DIMENSIONS OF 961HA FERRULED COUPLED-CAVITY TRAVELING-WAVE-TUBE CIRCUIT

[See fig. 1.]

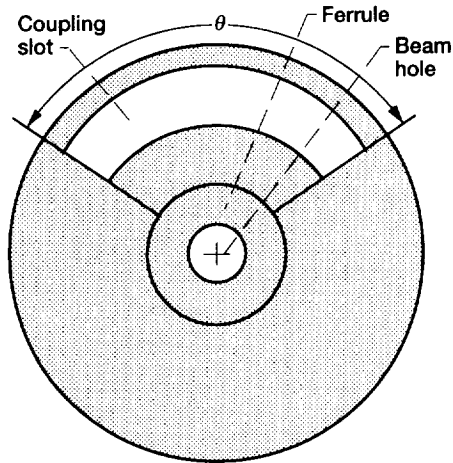
Ferrule radius, 10 ⁻³ m	
Inner, r_1	0.2794
Outer, r_2	0.4318
Slot radius, 10 ⁻³ m	
Inner, r_3	0.6858
Outer r_4	1.1049
Cavity radius, r_5 , 10 ⁻³ m	1.1049
Gap, 10 ⁻³ m	
Ferrule, g	0.2921
Cavity, h	0.7518
Wall thickness, t , 10 ⁻³ m	0.2159
Cavity length, L , 10 ⁻³ m	0.9677
Slot arc, θ , deg	140

Analysis

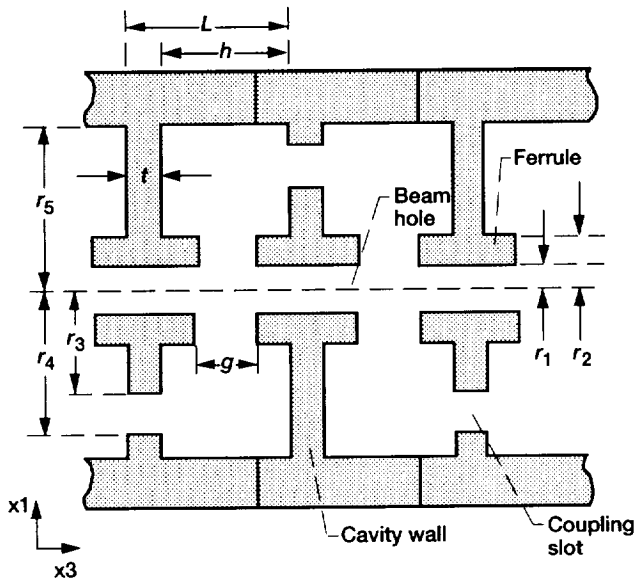
Dispersion Simulation

The frequency-phase dispersion characteristics of the ferruled coupled-cavity slow-wave circuit were obtained by modeling one- to four-cavity configurations of the structure. The frequency algorithm of Micro-SOS calculated the resonant frequencies for different values of phase shift per cavity to form an accurate dispersion curve. The different eigenmodes are forced by axially truncating the different cavity configurations with either an electric wall (simulated by using the STRUCTURE command) or a magnetic wall (simulated by using the SYMMETRY MIRROR command). An electric wall is a boundary that simulates a perfect conductor with the electric field perpendicular to the wall. At a magnetic wall boundary condition, the tangential magnetic field is zero and the magnetic field is perpendicular to the wall.

Truncating the longitudinal ends of the circuit with these boundary conditions corresponds to simulating standing waves with an integral number of half-wavelengths (phase



(a) End view.



(b) Top view.

Figure 1.—Generalized ferruled coupled-cavity, traveling wave tube (TWT) circuit.

shifts of π) in the length of the circuit. The cavity configurations and boundary conditions required for obtaining several resonant frequencies for the first forward RF space harmonic of the cavity mode and the first backward RF space harmonic of the slot mode using Micro-SOS are listed in table II (ref. 3). For each combination of cavity configuration and boundary conditions, the phase shifts per cavity for the resulting resonance frequencies are listed in the order of increasing frequency, with the slot-mode phase shifts enclosed in parentheses.

The total cavity-mode axial on-axis electric field $E_{z\text{tot}}$ is shown in figure 2 for each of the phase shifts per cavity listed in table II. The plots are extended over 12 cavities in order to show the full periodic nature of each case. The locations of the boundaries in the Micro-SOS simulations are shown by the

TABLE II.—BOUNDARY CONDITIONS FOR RESONANCE AT VARIOUS PHASE SHIFTS PER CAVITY

Number of cavities	Boundary conditions ^a	Phase shift per cavity, ^b βL , rad
1	MM	π ($2\pi, \pi$)
1	ME	$3\pi/2$ ($3\pi/2$)
1	EE	2π
2	ME	$5\pi/4, 7\pi/4$ ($7\pi/4, 5\pi/4$)
2	EE	$3\pi/2, 2\pi$
3	ME	$7\pi/6, 3\pi/2, 11\pi/6$ ($11\pi/6, 3\pi/2, 7\pi/6$)
3	EE	$4\pi/3, 5\pi/3, 2\pi$ ($5\pi/3, 4\pi/3$)
4	EE	$5\pi/4, 3\pi/2, 7\pi/4, 2\pi$ ($7\pi/4, 3\pi/2, 5\pi/4$)

^aMagnetic wall, M; electric wall, E.

^bSlot-mode phase shifts are in parentheses.

vertical truncation lines in figure 2, with electric and magnetic walls indicated by solid and dashed lines, respectively.

Because of the relatively small coupling slot size in this coupled-cavity circuit, the slot mode (which is technically a separate passband in the same mode as the cavity-mode passband) is at a higher frequency than the cavity mode (refs. 5 and 8). The axial electric field distribution near the axis is similar to that of the cavity mode at the same value of phase shift per cavity, except at 2π where the axial electric field is zero at the axis. The slot mode is characterized by a strong radial component of the electric field in some or all of the coupling slots.

A generalized input file was developed so that the resonant frequencies could be determined for any ferruled coupled-cavity TWT slow-wave circuit. As listed in the appendix, the file simulates four cavities with two electric walls. However, the file can be easily modified to simulate one, two, or three cavities with any of the three boundary condition combinations. The number of cavities modeled N is defined by the user in the CAVITY NUMBER section of the appendix; the boundary conditions can be adjusted by editing the SYMMETRY section.

In the generalized input file listed in the appendix, the grid is defined with the X1GRID, X2GRID, and X3GRID commands which refer to the radial, azimuthal, and axial directions, respectively. To model general ferruled coupled-cavity circuits in addition to that of the model 961HA TWT of this report, DEFINE commands are used frequently throughout the input file of the appendix. By exercising the DEFINE

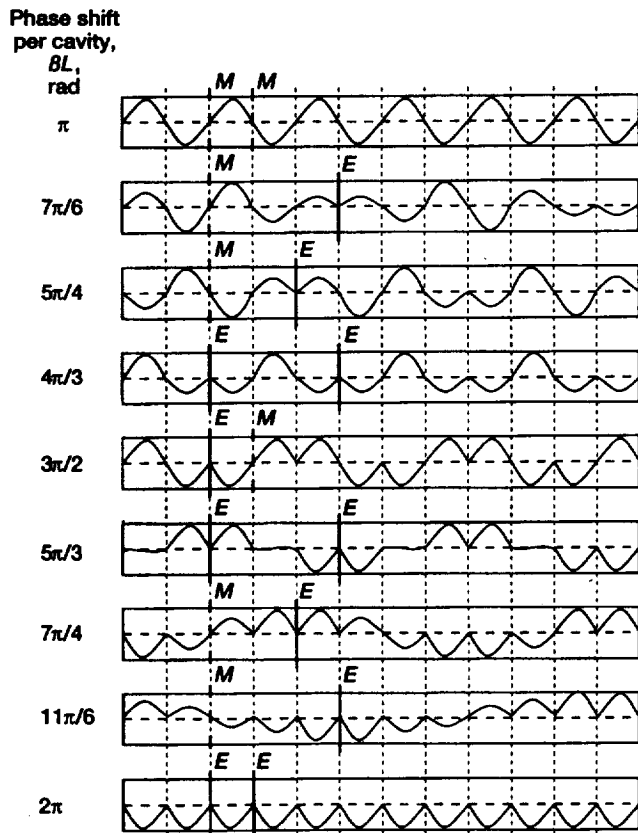
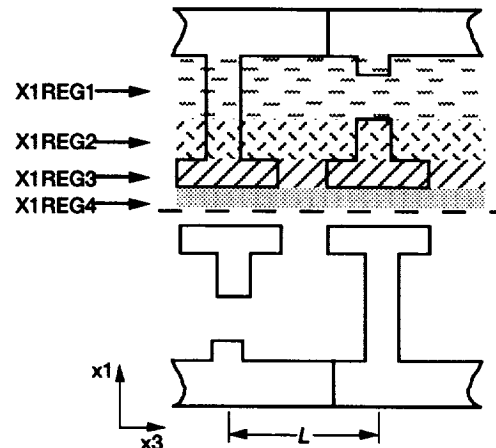


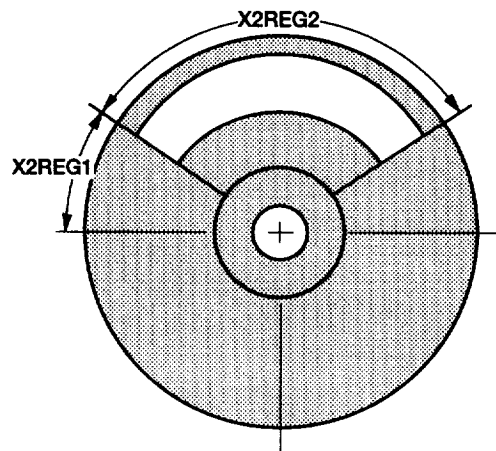
Figure 2.—Total axial on-axis electric field over 12 cavities with indicated boundary conditions (magnetic wall, M; electric wall, E).

command option, it is possible to specify the entire input file in terms of variable names. The CONVERT command used in the PARAMETER section of the appendix converts the dimensions of the cavity from inches to meters and simultaneously assigns that dimension to a variable name. If the user wishes to enter the dimensions originally in meters, the CONVERT commands can be replaced with DEFINE commands (ref. 2).

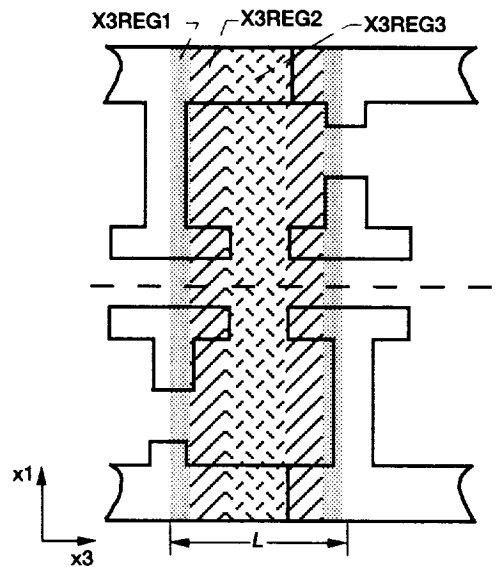
This generalized input file allows the user some freedom to experiment with various dimensions by changing the parameter dimensions in the PARAMETER section. It also allows experimentation with the grid spacings. Serving as a guide for the GRID SPACING section, figures 3(a) to (c) show views of one cavity of the ferruled coupled-cavity structure with the x_1 -, x_2 -, and x_3 -directions divided into regions. In this section, one can select a grid spacing for each of these regions. The file gives default values which have been proven to provide accurate results for the slow-wave circuit of the 961HA TWT.



(a) Radial direction x_1 .



(b) Azimuthal direction x_2 .



(c) Axial direction x_3 .

Figure 3.—Generalized ferruled coupled-cavity TWT circuit simulation segments.

Impedance Simulation

For each value of phase shift per cavity on the dispersion curve, the Pierce on-axis interaction impedance for the n^{th} RF space harmonic (ref. 9) is defined as

$$K_n = \frac{E_n^2}{2\beta_n^2 P_{RF}} \quad (1)$$

where E_n is the on-axis electric field magnitude of the n^{th} harmonic, β_n is the axial phase constant of the n^{th} harmonic defined by

$$\beta_n = \frac{\phi + 2\pi n}{L} \quad (2)$$

where ϕ is the phase shift per cavity in radians of the fundamental harmonic, n is the space harmonic order, L is the length of one cavity, and P_{RF} is the RF power flow defined by

$$P_{RF} = W v_g \quad (3)$$

where v_g is the group velocity, and W is the stored electromagnetic energy per unit length,

$$W = \frac{W_T}{NL} \quad (4)$$

with the total energy W_T calculated with Micro-SOS in the number of cavities simulated N . Thus, the Pierce on-axis interaction impedance can be expressed as

$$K_n = \frac{E_n^2 NL}{2\beta_n^2 W_T v_g} \quad (5)$$

In the typical ferruled coupled-cavity TWT circuit, the beam is synchronous only with the first RF space harmonic. Thus, we need to calculate only the first ($n = 1$) harmonic term in equation (5). To determine its magnitude E_1 , a Fourier analysis is performed on the total on-axis axial electric field $E_{z\text{tot}}$, which is tabulated at the center of each grid space along the axis in the z -direction by using the LINPRINT command.

In the analysis, the total axial electric field on the axis can be represented in terms of a Fourier series,

$$E_{z\text{tot}} = \sum_{-\infty}^{\infty} a_n \cos(\beta_n z) + b_n \sin(\beta_n z) \quad (6)$$

with

$$a_n = \frac{2}{P} \int_{-\frac{P}{2}}^{\frac{P}{2}} E_{z\text{tot}} \cos(\beta_n z) dz \quad (7)$$

and

$$b_n = \frac{2}{P} \int_{-\frac{P}{2}}^{\frac{P}{2}} E_{z\text{tot}} \sin(\beta_n z) dz \quad (8)$$

where P is the period of $E_{z\text{tot}}$. By defining $z = 0$ at a boundary, $E_{z\text{tot}}$ will always be either an even or an odd function with respect to z . If $z = 0$ at an electric wall, $E_{z\text{tot}}$ is an even function with $b_n = 0$, and the magnitude of the first harmonic is obtained from equation (7):

$$E_1 = \frac{4}{P} \int_0^{\frac{P}{2}} E_{z\text{tot}} \cos(\beta_1 z) dz \quad (9)$$

If $z = 0$ at a magnetic wall, $E_{z\text{tot}}$ is an odd function with $a_n = 0$, and the magnitude of the first harmonic is obtained from equation (8):

$$E_1 = \frac{4}{P} \int_0^{\frac{P}{2}} E_{z\text{tot}} \sin(\beta_1 z) dz \quad (10)$$

The group velocity of equation (5) is defined as

$$v_g = \frac{d\omega}{d\beta_1} \quad (11)$$

and is extracted from the dispersion curve which is plotted with frequency f (in gigahertz given by Micro-SOS) versus βL (in radians). Using these parameters, v_g can be expressed as

$$v_g = 2\pi L \frac{df}{d(\beta_1 L)} \quad (12)$$

Finally, to obtain W_T for equation (5), the BALANCE command is used to control the Micro-SOS energy calculation. The OBSERVE command is then used to record the specified variables during simulation. By specifying ENERGY and TOTAL in the OBSERVE command and designating the entire volume of the structure, the total electromagnetic energy W_T is obtained.

Results

The ferruled coupled-cavity slow-wave circuit of the model 961HA TWT was modeled in both the Cartesian and cylindrical coordinate systems. The results from these simulations were then compared with experimental results.

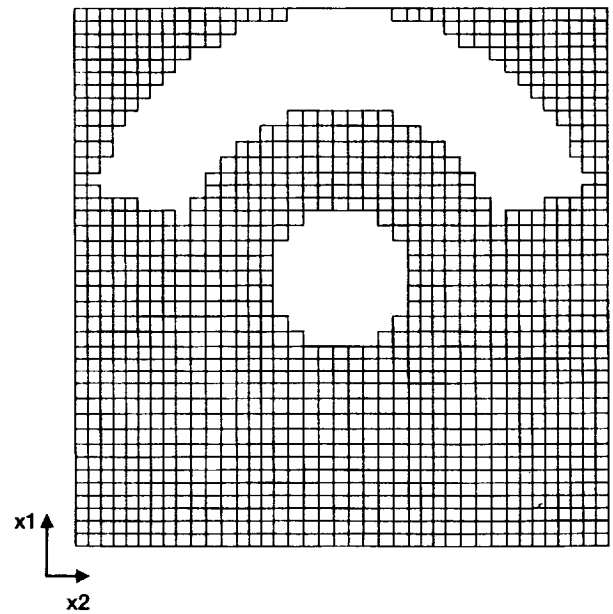
Dispersion Simulations

The Cartesian model was developed first. The Aug89SOS version of Micro-SOS (refs.1 to 3) was used to generate a grid cell resolution of 39 by 39 in the transverse plane and 13 per cavity in the longitudinal direction. Figures 4(a) and (b), which were generated by Micro-SOS, show the grid only in the conductor regions. The lines of the mesh were spaced as equally as possible and grid boundaries were matched with major geometrical features such as the beam hole and ferrules. The resonant frequencies obtained by modeling one and two cavities are compared with experimental data for the cavity mode in figure 5 and in table III.

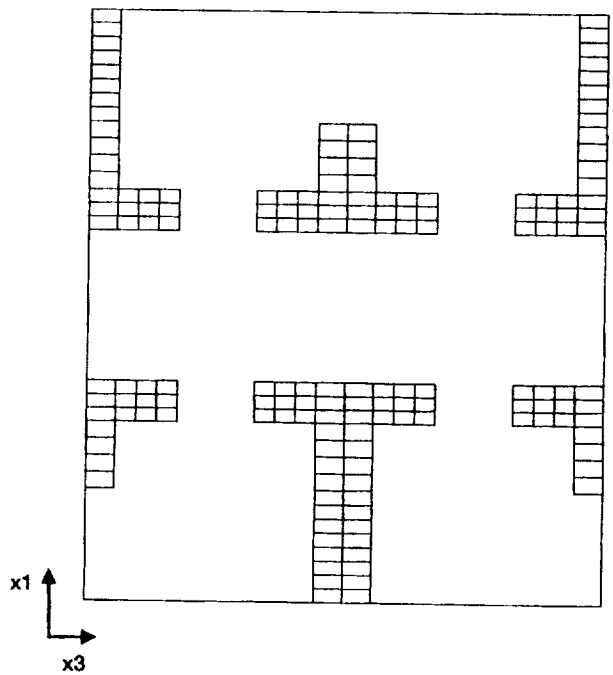
TABLE III.—CAVITY-MODE RESONANT FREQUENCIES FOR 961HA USING CARTESIAN COORDINATES

Phase shift per cavity, βL , rad	Experimental frequency, f , GHz	Micro-SOS frequency, f , GHz	Frequency difference Δf , percent
π	-----	52.53	-----
$5\pi/4$	55.88	54.67	-2.17
$3\pi/2$	61.38	60.35	-1.68
$7\pi/4$	69.87	68.30	-2.25
2π	75.47	74.48	-1.31

In comparison with data provided by the manufacturer (H.C. Limburg, 1992, Hughes Aircraft Co., Torrance, CA, personal communication), the Micro-SOS results using the Cartesian model were consistently lower by an average of 1.85 percent. Increasing the resolution of the grid resulted in only a slight reduction of the difference at the cost of increased computation time. It should be noted that in reference 3 the calculated resonance frequencies were reported to be consistently lower than the experimental results by about 4 percent for a similar ferruled coupled-cavity TWT.



(a) End view.



(b) Top view.

Figure 4.—Micro-SOS grid for 961HA ferruled coupled-cavity TWT circuit over two cavities.

To determine if more accurate results could be obtained, the ferruled coupled-cavity slow-wave circuit was also modeled in cylindrical coordinates with a grid resolution of 13 by 18 by 13 per cavity in the radial, azimuthal, and axial directions, respectively. Again, the grid lines were spaced as equally as possible while the grid boundaries were kept coincident with all surfaces.

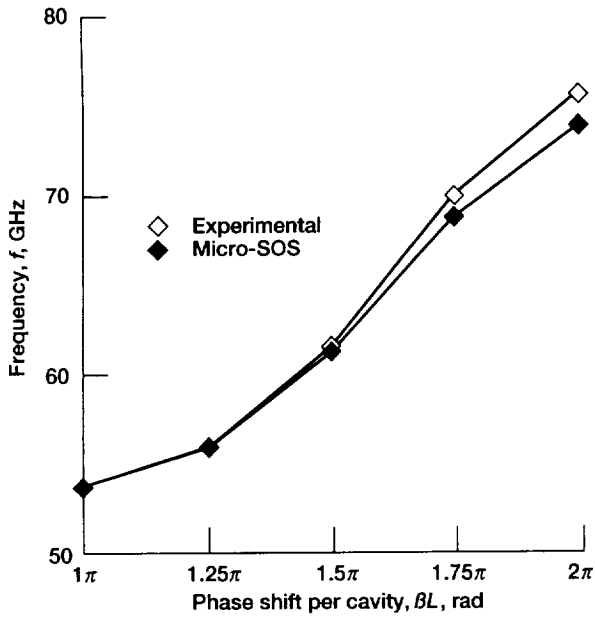


Figure 5.—Experimental and Micro-SOS Cartesian coordinate simulation of dispersion for cavity mode of 961HA TWT.

Results for the dispersion curve simulated with one-, two-, and three-cavity configurations in the cylindrical coordinate system are shown in figure 6 and are presented in tables IV and V for the cavity and slot modes. Compared with the experimental data, the cavity-mode results agree within 0.37 percent for the lower frequency resonances of the

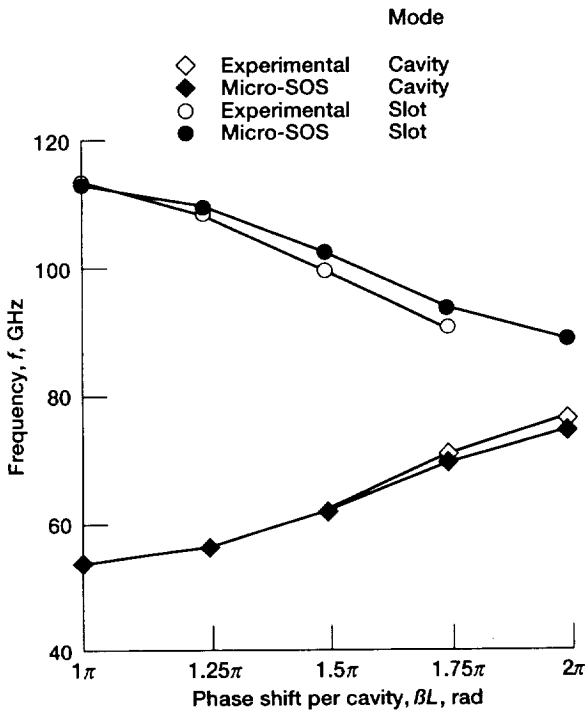


Figure 6.—Experimental and Micro-SOS cylindrical coordinate simulations of dispersion for cavity and slot modes of 961HA TWT.

TABLE IV.—CAVITY-MODE RESONANT FREQUENCIES FOR 961HA TRAVELING WAVE TUBE USING CYLINDRICAL COORDINATES

Phase shift per cavity, βL , rad	Experimental frequency, f , GHz	Micro-SOS frequency, f , GHz	Frequency difference Δf , percent
π	-----	53.69	-----
$7\pi/6$	54.44	54.64	+0.37
$5\pi/4$	55.88	55.74	-.25
$3\pi/2$	61.38	61.18	-.33
$7\pi/4$	69.87	68.59	-1.83
$11\pi/6$	72.03	71.00	-1.43
2π	75.47	73.68	-2.37

TABLE V.—SLOT-MODE RESONANT FREQUENCIES FOR 961HA TRAVELING WAVE TUBE USING CYLINDRICAL COORDINATES

Phase shift per cavity, βL , rad	Experimental frequency, f , GHz	Micro-SOS frequency, f , GHz	Frequency difference Δf , percent
π	-----	112.83	-----
$7\pi/6$	112.71	111.08	-1.45
$5\pi/4$	110.91	109.37	-1.39
$3\pi/2$	102.98	101.81	-1.14
$7\pi/4$	93.25	92.86	-0.42
$11\pi/6$	90.30	90.16	-0.16
2π	-----	87.72	-----

dispersion curve, but for increasing frequencies, the differences increase significantly to -2.37 percent for a phase shift per cavity of 2π . The Micro-SOS cylindrical results were significantly closer to the experimental results with an average absolute frequency difference of only 1.10 percent, compared to the Cartesian results with the average difference being 1.85 percent. Increasing the grid resolution did not significantly reduce the difference. The Micro-SOS results for the slot mode agree very well with the experimental data with an average absolute frequency difference of 0.91 percent.

Impedance Simulation

The Pierce on-axis interaction impedance for the first forward space harmonic was calculated from equation (5) using the Micro-SOS cylindrical model dispersion simulation results. The impedance results are shown in figure 7 and table VI. As shown, the impedance values match very well, especially for the lower values of phase shift, with an average absolute difference of 3.09 percent when compared with experimental cold-test results.

TABLE VI.—PIERCE ON-AXIS INTERACTION
IMPEDANCE

Phase shift per cavity, βL , rad	Experimental impedance, K_1 , Ω	Micro-SOS impedance, K_1 , Ω	Impedance difference ΔK , percent
$5\pi/4$	23.85	23.83	-0.08
$4\pi/3$	14.56	14.62	0.41
$3\pi/2$	7.09	7.32	3.24
$5\pi/3$	4.26	4.59	7.75
$7\pi/4$	3.53	3.67	3.97

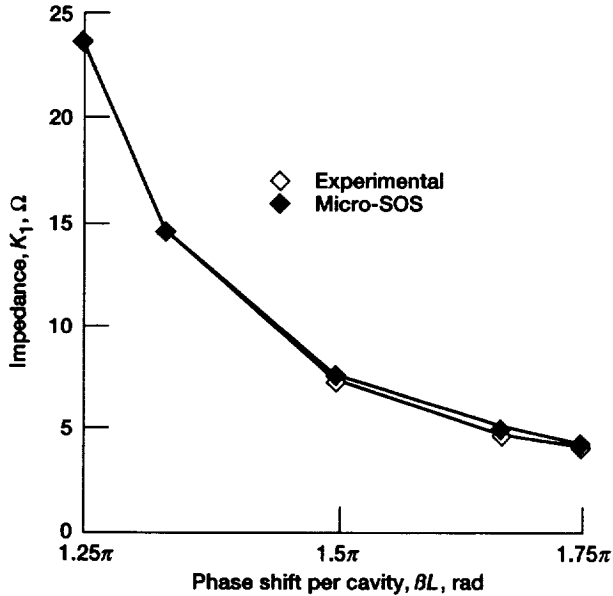


Figure 7.—Experimental and Micro-SOS cylindrical coordinate simulation of Pierce on-axis interaction impedance for 961HA TWT.

Conclusions

A generalized ferruled coupled-cavity traveling-wave-tube (TWT) circuit input file was developed for the three-dimensional electromagnetic circuit analysis code Micro-SOS. Arbitrary circuit geometries can be easily modeled by simply adjusting dimensions in the file. The use of the file for the accurate generation of the frequency-phase dispersion and Pierce on-axis interaction impedance characteristics was detailed.

The generalized input file was used to simulate the dispersion and impedance for a specific circuit, that of the 961HA coupled-cavity TWT. The agreement with experiment was very good with an average absolute frequency difference of about 1 percent and an average absolute impedance difference of about 3 percent. These results demonstrate the reliability of Micro-SOS simulations and their capability to reduce expensive and time-consuming experimental procedures in the design process for coupled-cavity TWT's.

Lewis Research Center
National Aeronautics and Space Administration
Cleveland, Ohio
October 4, 1993

APPENDIX—Micro-SOS Input File

```
TITLE * GENERALIZED INPUT FILE FOR A FERRULED COUPLED-CAVITY CIRCUIT
      IN CYLINDRICAL COORDINATES * /

SYSTEM CYLINDRICAL /

C ***** /
C PARAMETER SECTION...PARAMETER SECTION... PARAMETER SECTION... /
C ***** /
COMMENT * CONVERT AND DEFINE DIMENSIONS, DIMENSIONS LISTED ARE FOR THE
      HUGHES 961HA CIRCUIT * /

COMMENT * FERRULE INNER RADIUS = r1 * /
CONVERT RBEAMHOLE 0.0110 INCHES /

COMMENT * FERRULE OUTER RADIUS = r2 * /
CONVERT RFERRULE 0.0170 INCHES /

COMMENT * SLOT INNER RADIUS = r3 * /
CONVERT RPATCH 0.0270 INCHES /

COMMENT * SLOT OUTER RADIUS = r4 * /
CONVERT RSLOT 0.0435 INCHES /

COMMENT * CAVITY RADIUS = r5 * /
CONVERT RCAVITY 0.0435 INCHES /

COMMENT * FERRULE GAP = g * /
CONVERT FERRULESPACE 0.0115 INCHES /

COMMENT * CAVITY GAP = h * /
CONVERT CAVITYSPACE 0.0296 INCHES /

COMMENT * WALL THICKNESS = t * /
CONVERT WALLTHICK 0.0085 INCHES /

COMMENT * PERIOD LENGTH = L * /
CONVERT CAVITYLENGTH 0.0381 INCHES /

COMMENT * SLOT ARC = theta * /
DEFINE SLOTARC 140 /

DEFINE PI 3.14159265359 /
C ***** /
C ***** /

C ***** /
C CAVITY NUMBER SECTION...CAVITY NUMBER SECTION...CAVITY NUMBER SECTION... /
C ***** /
COMMENT * DEFINE THE NUMBER OF CAVITIES TO BE MODELED, N * /

DEFINE N 4 /
C ***** /
C ***** /

C ***** /
C GRID SPACING SECTION...GRID SPACING SECTION...GRID SPACING SECTION... /
C ***** /
COMMENT * FOLLOW FIGURES 3a, b AND c FOR REGIONS * /

DEFINE X1REG1 4 /
DEFINE X1REG2 3 /
DEFINE X1REG3 2 /
DEFINE X1REG4 4 /
```

```

DEFINE X2REG1 1 /
DEFINE X2REG2 7 /

DEFINE X3REG1 1 /
DEFINE X3REG2 3 /
DEFINE X3REG3 5 /
C ***** /
C ***** /

DEFINE CAVSTART CAVITYLENGTH CAVITYSPACE SUBTRACT 2.0 DIVIDE /

DEFINE LENGTH CAVITYLENGTH N MULTIPLY /

DEFINE X1MAX RCAVITY /
DEFINE X1MIN 0 /
DEFINE X2MAX PI 2.0 MULTIPLY /
DEFINE X2MIN 0 /
DEFINE X3MAX LENGTH 2 DIVIDE /
DEFINE X3MIN X3MAX -1 MULTIPLY /

DEFINE X1TOTGRID X1REG1 X1REG2 ADD X1REG3 ADD X1REG4 ADD 1 ADD /
DEFINE X2TOTGRID X2REG1 4 MULTIPLY X2REG2 ADD X2REG2 ADD 1 ADD /
DEFINE X3PER X3REG1 X3REG2 ADD X3REG3 ADD X3REG2 ADD X3REG1 ADD /
DEFINE X3TOTGRID X3PER N MULTIPLY 1 ADD /

DEFINE X1BLOCK X1TOTGRID 1 ADD /
DEFINE X2BLOCK X2TOTGRID 1 ADD /
DEFINE X3BLOCK X3TOTGRID 1 ADD /

DEFINE X1SPACE1 RCAVITY RPATCH MINUS X1REG1 DIVIDE /
DEFINE X1SPACE2 RPATCH RFERRULE MINUS X1REG2 DIVIDE /
DEFINE X1SPACE3 RFERRULE RBEAMHOLE MINUS X1REG3 DIVIDE /
DEFINE X1SPACE4 RBEAMHOLE X1REG4 DIVIDE /

DEFINE X1DIM1 X1SPACE1 X1REG1 MULTIPLY /
DEFINE X1DIM2 X1SPACE2 X1REG2 MULTIPLY /
DEFINE X1DIM3 X1SPACE3 X1REG3 MULTIPLY /
DEFINE X1DIM4 X1SPACE4 X1REG4 MULTIPLY /

DEFINE X2DIM2 SLOTARC PI MULTIPLY 180 DIVIDE /
DEFINE X2DIM1 PI X2DIM2 MINUS 2 DIVIDE /

DEFINE X2SPACE1 X2DIM1 X2REG1 DIVIDE /
DEFINE X2SPACE2 X2DIM2 X2REG2 DIVIDE /

DEFINE X3SPACE1 CAVSTART X3REG1 DIVIDE /
DEFINE FERRHEIGHT CAVITYLENGTH FERRULESPACE MINUS 2 DIVIDE CAVSTART MINUS /
DEFINE X3SPACE2 FERRHEIGHT X3REG2 DIVIDE /
DEFINE X3SPACE3 FERRULESPACE X3REG3 DIVIDE /

DEFINE X3DIM1 CAVSTART /
DEFINE X3DIM2 X3SPACE2 X3REG2 MULTIPLY /
DEFINE X3DIM3 X3SPACE3 X3REG3 MULTIPLY /

X1GRID FUNCTION X1TOTGRID 1 X1MIN X1REG4 X1SPACE4 X1DIM4
X1REG3 X1SPACE3 X1DIM3
X1REG2 X1SPACE2 X1DIM2
X1REG1 X1SPACE1 X1DIM1 /

X2GRID FUNCTION X2TOTGRID 1 X2MIN X2REG1 X2SPACE1 X2DIM1
X2REG2 X2SPACE2 X2DIM2
X2REG1 X2SPACE1 X2DIM1
X2REG1 X2SPACE1 X2DIM1
X2REG2 X2SPACE2 X2DIM2

```

```

X2REG1 X2SPACE1 X2DIM1 /
X3GRID FUNCTION X3TOTGRID 1 X3MIN X3REG1 X3SPACE1 X3DIM1
X3REG2 X3SPACE2 X3DIM2
X3REG3 X3SPACE3 X3DIM3
X3REG2 X3SPACE2 X3DIM2
X3REG1 X3SPACE1 X3DIM1
X3REG1 X3SPACE1 X3DIM1
X3REG2 X3SPACE2 X3DIM2
X3REG3 X3SPACE3 X3DIM3
X3REG2 X3SPACE2 X3DIM2
X3REG1 X3SPACE1 X3DIM1
X3REG1 X3SPACE1 X3DIM1
X3REG2 X3SPACE2 X3DIM2
X3REG3 X3SPACE3 X3DIM3
X3REG2 X3SPACE2 X3DIM2
X3REG1 X3SPACE1 X3DIM1
X3REG1 X3SPACE1 X3DIM1
X3REG2 X3SPACE2 X3DIM2
X3REG3 X3SPACE3 X3DIM3
X3REG2 X3SPACE2 X3DIM2
X3REG1 X3SPACE1 X3DIM1 /

C ***** /
C SYMMETRY SECTION...SYMMETRY SECTION...SYMMETRY SECTION... /
C ***** /
SYMMETRY AXIAL +1 1 1 1 X2TOTGRID 1 X3TOTGRID /
SYMMETRY PERIODIC +1 1 X1TOTGRID 1 1 1 X3TOTGRID
ANTI-ALIGN 1 X1TOTGRID X2TOTGRID X2TOTGRID 1 X3TOTGRID /

COMMENT * SEE TABLE II. FOR BOUNDARY/CAVITY CONFIGURATIONS.
2 SYMMETRY PLANES SIMULATE THE MM BOUNDARY CONDITION,
COMMENTING OUT 1 SYMMETRY SIMULATES AN EM BOUNDARY CONDITION,
COMMENTING OUT BOTH SYMMETRY PLANES SIMULATES AN EE BOUNDARY * /
C SYMMETRY MIRROR ALIGN 1 X1TOTGRID 1 X2TOTGRID 1 1 /
C SYMMETRY MIRROR ANTI-ALIGN 1 X1TOTGRID 1 X2TOTGRID X3TOTGRID X3TOTGRID /
C ***** /
C ***** /

STRUCTURE CONFORMAL SOLIDIFY +1 1 X1BLOCK 1 X2TOTGRID 0 X3BLOCK /
STRUCTURE CONFORMAL CAVITY -1 1 X1TOTGRID 1 X2TOTGRID 1 X3TOTGRID /

DEFINE IFERRST X1REG4 1 ADD /
DEFINE IFERREN IFERRST X1REG3 ADD /
STRUCTURE CONFORMAL FERRULE +1 IFERRST IFERREN 1 X2TOTGRID 1 X3TOTGRID /

C ***** /
C WALL SECTION...WALL SECTION...WALL SECTION...WALL SECTION... /
C ***** /
COMMENT * FORM THE WALLS * /

DEFINE LEND X3REG1 1 ADD /
STRUCTURE CONFORMAL LWALL +1 IFERREN X1TOTGRID 1 X2TOTGRID 1 LEND /

DEFINE RST X3TOTGRID X3REG1 MINUS /
STRUCTURE CONFORMAL RWALL +1 IFERREN X1TOTGRID 1 X2TOTGRID RST X3TOTGRID /

DEFINE N1 N 1 MINUS /

COMMENT * FORM THE CENTER WALLS * /
DO K 1 N1 1 /

```

```

DEFINE MIEND LEND X3PER K MULTIPLY ADD /
DEFINE M1ST MIEND X3REG1 MINUS X3REG1 MINUS /
STRUCTURE CONFORMAL MWALLN +1 IFERREN X1TOTGRID 1 X2TOTGRID M1ST MIEND /

ENDDO /
C ***** /
C ***** /

C ***** /
C SLOT SECTION...SLOT SECTION...SLOT SECTION...SLOT SECTION... /
C ***** /
COMMENT * FORM THE SLOTS * /

DEFINE ISLOTST IFERREN X1REG2 PLUS /
DEFINE SLRST X2REG1 1 ADD /
DEFINE SLREND SLRST X2REG2 ADD /
DEFINE SLLST SLREND X2REG1 ADD X2REG1 ADD /
DEFINE SLEND SLLST X2REG2 ADD /
ENGRID X1 ISLOTEND RSLST /
DEFINE ISLOTEND ISLOTEND 1 ADD /

STRUCTURE CONFORMAL SLOTRT -1 ISLOTST ISLOTEND SLRST SLREND 1 LEND /

DO K 1 N 2 /

DEFINE MIEND LEND X3PER K MULTIPLY ADD /
DEFINE M1ST MIEND X3REG1 MINUS X3REG1 MINUS /
STRUCTURE CONFORMAL SLOTRT -1 ISLOTST ISLOTEND SLLST SLEND M1ST MIEND /

ENDDO /

DO K 2 N 2 /

DEFINE MIEND LEND X3PER K MULTIPLY ADD /
DEFINE M1ST MIEND X3REG1 MINUS X3REG1 MINUS /
STRUCTURE CONFORMAL SLLT -1 ISLOTST ISLOTEND SLRST SLREND M1ST MIEND /

ENDDO /

COMMENT * FILL IN THE PORTION THE SLOT HOLLOWED OUT IN THE CONDUCTING WALL
AT THE AXIAL END * /
STRUCTURE CONFORMAL SLPATCH +1 1 X1TOTGRID 1 X2TOTGRID X3TOTGRID X3BLOCK /
C ***** /
C ***** /

C ***** /
C GAP SECTION...GAP SECTON...GAP SECTION...GAP SECTION...GAP SECTION... /
C ***** /
COMMENT * FORM THE GAP * /
DO K 0 N1 1 /

DEFINE GAP1ST X3REG1 X3REG2 ADD 1 ADD X3PER K MULTIPLY ADD /
DEFINE GAP1END GAP1ST X3REG3 ADD /
STRUCTURE CONFORMAL GAP1 -1 IFERRST IFERREN 1 X2TOTGRID GAP1ST GAP1END /

ENDDO /
C ***** /
C ***** /

C ***** /
C DIAGNOSTIC SECTION...DIAGNOSTIC SECTION...DIAGNOSTIC SECTION... /
C ***** /
GRAPHICS SYSTEM /

```

```
C DISPLAY MODEL 2 2 /
C DISPLAY MODEL 2 12 /

DIAGNOSE FREQUENCY 1 0 4 /

FREQUENCY 4 150E+9 .001 50000 /

RANGE 1 1 0.0 0.0 E3 1 1 1 1 1 X3TOTGRID /

LINPRINT 1 X3 X1 1 1 1 1 1 X3TOTGRID 0 0 1 0 0 0 0 0 0 /

BALANCE 1 1 X1TOTGRID 1 X2TOTGRID 1 X3TOTGRID /
OBSERVE 1 YES ENERGY 1 0.0 0.0 0.0 0.0 TOTAL 0 1 /
C ***** /
C ***** /

START /
STOP /
```

References

1. Goplen, B.; McDonald, J.; and Warren, G.: SOS Reference Manual Version October 1988, Mission Research Corporation, Newington, VA, Mar. 1989.
2. Goplen, B., et al.: SOS User's Manual Version October 1988, Mission Research Corporation, Newington, VA, Mar. 1989.
3. Doniger, K., et al.: Standard Problem Set for Micro-SOS Electromagnetic Circuit Modeling Code Version October 1988, Varian Associates, Inc., Palo Alto, CA, Mar. 1989.
4. Wilson, J.D.: Revised NASA Axially Symmetric Ring Model for Coupled-Cavity Traveling-Wave Tubes. NASA TP-2675, 1987.
5. Kantrowitz, F.; and Tammaru, I.: Three-Dimensional Simulations of Frequency-Phase Measurements of Arbitrary Coupled-Cavity RF Circuits, IEEE Trans. Electron Devices, vol. 35, no. 11, Nov. 1988, pp. 2018-2026.
6. Wilson, J.D., et al.: A High-Efficiency 59 to 64 GHz TWT for Intersatellite Communications. IEDM, Technical Digest: International Electron Devices Meeting, IEEE, Washington, D.C., 1991, pp. 585-588.
7. Rousseau, A.L.; Tammaru, I.; and Vaszari, J.P.: Development of a 75-Watt 60-GHz Traveling-Wave Tube for Intersatellite Communications. NASA CR-182135, 1988.
8. Gittins, J.F.: Power Traveling-Wave Tubes. Elsevier Publishing Company, Inc., New York, 1965.
9. Pierce, J.R.: Traveling-Wave Tubes. Van Nostrand, New York, 1950.



REPORT DOCUMENTATION PAGE			Form Approved OMB No. 0704-0188	
Public reporting burden for this collection of information is estimated to average 1 hour per response, including the time for reviewing instructions, searching existing data sources, gathering and maintaining the data needed, and completing and reviewing the collection of information. Send comments regarding this burden estimate or any other aspect of this collection of information, including suggestions for reducing this burden, to Washington Headquarters Services, Directorate for Information Operations and Reports, 1215 Jefferson Davis Highway, Suite 1204, Arlington, VA 22202-4302, and to the Office of Management and Budget, Paperwork Reduction Project (0704-0188), Washington, DC 20503.				
1. AGENCY USE ONLY (Leave blank)	2. REPORT DATE November 1993	3. REPORT TYPE AND DATES COVERED Technical Paper		
4. TITLE AND SUBTITLE Generalized Three-Dimensional Simulation of Ferruled Coupled-Cavity Traveling-Wave-Tube Dispersion and Impedance Characteristics			5. FUNDING NUMBERS WU-506-72	
6. AUTHOR(S) Joseph W. Maruschek, Carol L. Kory, and Jeffrey D. Wilson				
7. PERFORMING ORGANIZATION NAME(S) AND ADDRESS(ES) National Aeronautics and Space Administration Lewis Research Center Cleveland, Ohio 44135-3191			8. PERFORMING ORGANIZATION REPORT NUMBER E-7977	
9. SPONSORING/MONITORING AGENCY NAME(S) AND ADDRESS(ES) National Aeronautics and Space Administration Washington, D.C. 20546-0001			10. SPONSORING/MONITORING AGENCY REPORT NUMBER NASA TP-3389	
11. SUPPLEMENTARY NOTES Joseph W. Maruschek, Ohio Aerospace Institute, 22800 Cedar Point Road, Brook Park, Ohio 44142; Carol L. Kory, Analex Corporation, 3001 Aerospace Parkway, Brook Park, Ohio 44142; and Jeffrey D. Wilson, NASA Lewis Research Center, Cleveland, Ohio. Responsible person, Jeffrey D. Wilson, (216) 433-3513.				
12a. DISTRIBUTION/AVAILABILITY STATEMENT Unclassified - Unlimited Subject Category 33			12b. DISTRIBUTION CODE	
13. ABSTRACT (Maximum 200 words) The frequency-phase dispersion and Pierce on-axis interaction impedance of a ferruled coupled-cavity traveling-wave-tube (TWT) slow-wave circuit were calculated using the three-dimensional simulation code Micro-SOS. The utilization of the code to reduce costly and time-consuming experimental cold tests is demonstrated by the accuracy achieved in calculating these parameters. A generalized input file was developed so that ferruled coupled-cavity TWT slow-wave circuits of arbitrary dimensions could be easily modeled. The practicality of the generalized input file was tested by applying it to the ferruled coupled-cavity slow-wave circuit of the Hughes Aircraft Company model 961HA TWT and by comparing the results with experimental results.				
14. SUBJECT TERMS Traveling wave tube; Coupled cavity; Dispersion; Impedance			15. NUMBER OF PAGES 16	
			16. PRICE CODE A03	
17. SECURITY CLASSIFICATION OF REPORT Unclassified	18. SECURITY CLASSIFICATION OF THIS PAGE Unclassified	19. SECURITY CLASSIFICATION OF ABSTRACT Unclassified	20. LIMITATION OF ABSTRACT	